Environmental Monitoring and Assessment (2006) **114:** 65–83
DOI: 10.1007/s10661-006-1071-z

TEXTURE ANALYSIS FOR MAPPING *TAMARIX PARVIFLORA* USING AERIAL PHOTOGRAPHS ALONG THE CACHE CREEK, CALIFORNIA

SHAOKUI GE[1,2,*], RAYMOND CARRUTHERS[2], PENG GONG[1]
and ANGELICA HERRERA[1,2]

[1]*Department of Environmental Science, Policy, and Management, University of California, Berkeley, California, USA;* [2]*Exotic and Invasive Weeds Research Unit, Western Regional Research Center USDA, Agricultural Research Service, 800 Buchanan Street Albany, California, USA*

*(*author for correspondence, e-mail: gesk@nature.berkeley.edu)*

(Received 17 September 2004; accepted 24 January 2005)

Abstract. Natural color photographs were used to detect the coverage of saltcedar, *Tamarix parviflora*, along a 40 km portion of Cache Creek near Woodland, California. Historical aerial photographs from 2001 were retrospectively evaluated and compared with actual ground-based information to assess accuracy of the assessment process. The color aerial photos were sequentially digitized, georeferenced, classified using color and texture methods, and mosaiced into maps for field use. Eight types of ground cover (*Tamarix*, agricultural crops, roads, rocks, water bodies, evergreen trees, non-evergreen trees and shrubs (excluding *Tamarix*)) were selected from the digitized photos for separability analysis and supervised classification. Due to color similarities among the eight cover types, the average separability, based originally only on color, was very low. The separability was improved significantly through the inclusion of texture analysis. Six types of texture measures with various window sizes were evaluated. The best texture was used as an additional feature along with the color, for identifying *Tamarix*. A total of 29 color photographs were processed to detect *Tamarix* infestations using a combination of the original digital images and optimal texture features. It was found that the saltcedar covered a total of 3.96 km^2 (396 hectares) within the study area. For the accuracy assessment, 95 classified samples from the resulting map were checked in the field with a global position system (GPS) unit to verify *Tamarix* presence. The producer's accuracy was 77.89%. In addition, 157 independently located ground sites containing saltcedar were compared with the classified maps, producing a user's accuracy of 71.33%.

Keywords: invasive species, saltcedar, tamarix parviflora, monitoring, detection, aerial photograph, remote sensing, California, texture analysis

1. Introduction

Biological invasions have increasingly become an important topic for environmental scientists and natural resource managers, worldwide. Invasive species alter community composition and ecosystem function, and cause severe threats to biodiversity in the invaded areas. In order to understand the invasion mechanism and better control invasive plants and their spread, it is helpful to characterize the abundance and distribution of an invasive species in areas of concern (Mooney, 1999). Although ground-based investigation can accurately measure invasive species in a limited

area, it is a time-consuming, labor-intensive work. In particular, ground-based assessment is not always practical for inaccessible areas where invasive species often exist. Thus, remote sensing can be an important tool to detect and characterize invasive species over large areas (Everitt *et al*., 1995, 1996; Lass *et al*., 1996). Saltcedars, *Tamarix* spp., were introduced to the United States in the 1800's for a variety of reasons including soil and wind erosion control. This shrub escaped from cultivation and now poses a significant threat to the natural ecosystems in the western USA (Brock, 1994; Di Tomaso, 1998; Bailey *et al*., 2001). It grows most successfully along riparian zones, where it out-competes native vegetation.

This invasive shrub has spread widely along Cache Creek and other riparian areas in Northern California (Figure 1). Its roots extend deeply into the soil where it depletes surface and underground water. In addition to its extensive water use, its invasion causes several other negative impacts such as salinization of soils, high stream bank erosion, increased flooding and high fire hazard to localized habitats. Multiple stems and slender branches characterize the general morphology of saltcedar, which may grow over 10 meters in height (Figure 2). It out-competes and replaces native vegetation, resulting in high-density monospecific-stands of saltcedar along riparian corridors. In some areas, water consumption and salt

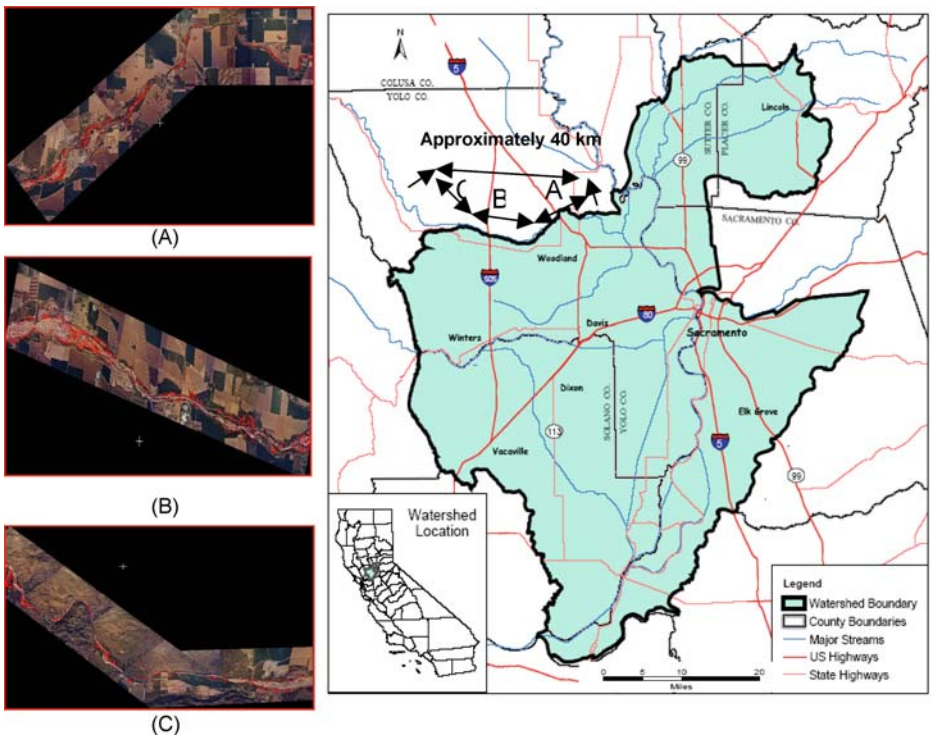

Figure 1. Study area (Cache Creek, California, USA, after California NRCS, (A) down part; (B) middle part; and (C) up part for this study).

Figure 2. Showing Saltcedars patches.

buildup have highly altered native ecosystems to the point that few other species can survive. It is therefore critical that effective techniques to limit saltcedar growth and control its spread be developed and implemented (Di Tomaso, 1998; Cleverly *et al*., 1997; Zavaleta, 2000; Bailey *et al*., 2001). Such attempts closely depend upon accurate detection of this plant on a regional scale, thus control actions can be applied widely throughout entire watersheds. However, except for some preliminary tests using digital videography, no research has been reported on the use of aerial photography in monitoring saltcedar distributions across wide areas or entire watersheds.

It was demonstrated that high spatial resolution remotely sensed data was a valuable data source to detect invasive species infestations across wide areas (Gausman *et al*., 1977; Everitt et al 1995; Lass *et al*., 1996). Wide area assessment is often important because invasive species are commonly distributed in an aggregated fashion providing a patchwork pattern in specific habitats within an invaded area. In particular, for invasive and noxious plant weed, small-patches of infested habitat are very important and cannot be ignored, since they often are newly infected areas under high-intensity control or eradication. Existing studies of invasive species have primarily been based on the reflectance difference of targets with the expectation that vegetation types could be distinguished from surrounding neighboring plants based on color or color infrared photographs (CIR). For example, having compared the application of color photos with CIR aerial photography, Everitt and Deloach (1990) found that the foliage of *Tamarix ramosissima* turned golden brown during the late fall/ early winter period so that its reflectance curve was much different from those of the associated native vegetation and soil background. Both types of photography (color and CIR) were used to distinguish *Tamarix ramosissima* from associated native vegetation. Color photography, however, is more widely available than CIR using both film and digital technology. High resolution commercial satellite images are usually taken along polar orbits with a narrow footprint. It takes multiple overpasses of those satellites to acquire images over a river system that could take many different directions in their meanderings. Therefore, the cost of

data acquisition is high. In consideration of these factors, color aerial photography was thought to be the most cost-effective remote sensing tool for the study of saltcedar in our riparian environment and several sets of historical photographs of Cache Creek were available.

In this study, color aerial photography was used to map invasive *Tamarix parviflora* along an east running portion of Cache Creek, near Woodland, California (see Figure 1). Traditionally, for specific feature extraction and delineation, manual photo interpretation is the most common method used by landmanagers interested in invasive plant control. However, manual interpretation is both time-consuming and labor-intensive, and it is almost impossible to recognize small patches of vegetation over wide areas or at a watershed scale of interest. Therefore, we developed an image based classification procedure to extract *Tamarix* covers for large areas along riparian corridors. Here, not only color but also image texture was used to detect these invasive plants. Texture analysis was considered important because color alone was not sufficient to separate *Tamarix* cover from adjacent beneficial plant species. In general, texture refers to the tonal variation in an image; and thus texture features help enhance separability among classes (Anys *et al*., 1995; Mather *et al*., 1998; Smits *et al*., 1999; Jonathan *et al*., 2001).

Texture extraction algorithms have been developed from remotely sensed data for various spatial resolutions (Haralick *et al*., 1973; Haralick, 1979; Gong *et al*., 1992; Hassan and He 1995; Riou *et al*., 1997; Saatchi *et al*., 2000, Nyoungui *et al*., 2002; Xu *et al*., 2003). All these studies demonstrated that texture in a local pixel neighborhood can be used to improve vegetation discrimination in high-resolution images (Hudak *et al*., 1998; Podest and Saatchi, 2002). In this paper we report our analysis methods and experimental results. In addition, we evaluate some commonly used texture measures for improving land cover classification from aerial color photographs and assess the accuracy of extracted *Tamarix parviflora* distributions through ground-based verification.

2. Materials and Methods

Historical aerial photographs were used retrospectively to assess saltcedar infestations along an important waterway in Northern California and then linked back to ground based validation sampling conducted following this analysis. The photographs were actually taken for assessing gravel distribution along Cache Creek but were timed such that they correspond with peak bloom and thus allowed an assessment of the saltcedar infestation in this area. A total of 29 color photos were taken along Cache Creek in April 2001 using a Zeiss RMK TOP 15 camera with a Zeiss Pleogon A3/4 lens. The camera was physically mounted in a twin-engine aerial platform that was piloted by American Aerial Survey, Inc. The scale of the photos was 1:12,000. At the time of photography, the saltcedar was not yet leafed out and only flowers were present on these plants. The flowers were pink in color, mak-

ing them distinctive from other associated riparian vegetation and other background materials in the study area. Because the photographs were taken in response to flowering, it was possible to mix saltcedar with some blooming fruit trees in adjacent agricultural orchards and thus careful discrimination between riparian zones and agricultural fields was needed to ensure that only saltcedar was extracted. Although it was possible to scan the photos in great detail, we chose to scanned the photos to 1 meter resolution. The scanned photos were georeferenced to 1-meter resolution Digital Ortho Quarter Quads (DOQQ) from USGS with a second order polynomial function. After classification, they were mosaiced together to provide a continuous photographic map. Based on the color similarity and relationships among various types of plants in the area, vegetation was initially divided into eight categories: saltcedar, evergreen trees, non-evergreen trees, shrubs, crops, bare fields and hills (including agriculture and rangeland), water bodies (including wetlands), rocks and roads. The procedure used for mapping the saltcedar cover is outlined in Figure 3. The image processing used to distinguish the tamarix from associated vegetation and other background substrates required four distinct steps: (1) Texture extraction using six algorithms; (2) Texture subset selection based on separability measured by Bhattacharya distances (BD, Shaban and Dikshit, 2001); (3) Best texture determination based on classification accuracy; and (4) A post-classification processing procedure, were used as the basis of invasive habitat determination. Following this classification procedure, the original eight categories were reduced to six categories, by merging rocks and roads with bare fields and hills. Individual classified photos were then mosaiced into three discrete sections of a 40km long portion of Cache Creek: the downstream, middle and up-stream segments of the riparian corridor. Finally, using completely random samples 100 points were extracted from these classified maps and used to conduct overall accuracy assessments, including calculating producer's and user's accuracies.

2.1. Comparing color separability

The original image was scanned in three layers (blue, green and red) using 8 bits per layer. Then, twenty 1-meter pixels of each cover type were randomly sampled from these digital images, and then was replicated three times. The color differences among land covers were determined using analysis of variance, and a Tukey's multiple range test was used to examine the statistical significance between means at a 0.95 probability level.

2.2. Texture measurements

Texture measurements were derived from the digitally processed photographs based on a gray level co-occurrence matrix (GLCM) (Gong *et al*., 1992; Jensen, 1996). GLCM is usually a probability matrix whose elements are indexed by gray-level values of any pixel-pair (a, b) at a fixed distance and angle in a pixel neighborhood.

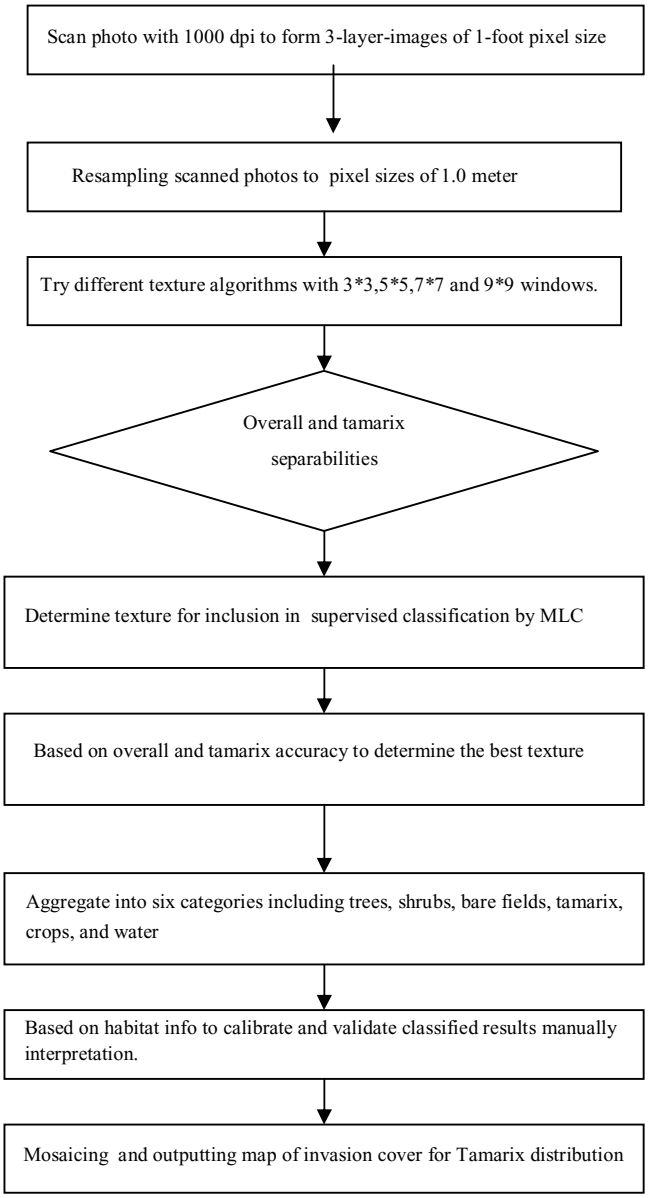

Figure 3. Procedures for the tamarix detection.

Given **N** as the number of gray levels and $P_{a,b}(i, j)$ as the joint probability of pixel a with gray level i and pixel b with gray level j. For each pixel neighborhood of a certain size, a GLCM was constructed with its ith row and jth column having probability $P_{a,b}(i, j)$. The relative spatial relationship between a and b is fixed for each GLCM. For simplicity, we will use P(i, j) instead of $P_{a,b}(i, j)$. The following

functions were used to develop texture algorithms:

$$\text{Homogeneity: } Homo = \sum \frac{p(i, j)}{1 + (i - j)^2} \tag{1}$$

$$\text{Contrast: } Con = \sum (i - j)^2 * p(i, j) \tag{2}$$

$$\text{Dissimilarity: } Dis = \sum p(i, j) * abs(i - j) \tag{3}$$

$$\text{Mean: } Mean = \sum i * p(i, j) \tag{4}$$

$$\text{Standard deviation: } Sdev = \sum p(i, j) * \left(i - \frac{\sum i}{n} \right)^2 \tag{5}$$

$$\text{Entropy: } Ent = -\sum p(i, j) \log p(i, j) \tag{6}$$

2.3. Between-class separability with different window sizes

Bhattacharya distance (BD) was applied to represent the separability between class pairs of training samples. BD values range between 0.0 and 2.00. If it is less than 1.00, the two cover classes are very similar and thus hard to separate. When this is the case, the classes should be merged or one of the cover classes discarded. BD values between 1.00 and 1.9 indicate that the two classes could be separated at least to some extent. BD values between 1.90 and 2.00 indicate very good separation between the two classes in question. In this study, texture measures were calculated and compared at different window sizes to determine the optimal window size for texture selection to distinguish invasive saltcedar from other surface covers. Comparisons were based on maximum, minimum and average separabilities of training samples with different texture measures obtained in window sizes of 3 * 3, 5 * 5, 7 * 7, and 9 * 9 pixels. A texture set was determined to be appropriate for classification when the separability was greater than 1.90. Specifically, the separability between *Tamarix* and other classes were given specific attention in order to determine whether it was separable from all other cover types. Based on the overall separability and *Tamarix* separability with each non-tamarix class, the optimal window size and texture feature were chosen for mapping tamarix the distribution along Cache Creek. This texture assessment was combined with the original image layers to jointly classify different pixel-based patterns to extract the invasive cover areas. Due to variation in light condition and topographical changes within our large study area, texture could be different from location to location, even for the same vegetation type. Therefore, in order to obtain accurate classification results, different textures were assessed and used across individual photos. As an example, a photo taken from the middle reach of the creek was used to illustrate such image processing.

2.4. Selection of the optimal texture algorithm

Various texture features selected as described previously, were added as additional channels to the original image classification process. The maximum likelihood classifier (MLC) was then used in the final classification, and class signatures were derived from images based on pixel color values and the selected texture determined by training samples. Although this study focused primarily on tamarix covers, the overall classification accuracy was still considered. Therefore, through the balanced assessment of the overall classification accuracy and the classification accuracy of tamarix, the optimal texture feature was selected for inclusion in the final classification.

2.5. Habitat-based calibration and accuracy assessment

Due to color similarities among different cover types, non-tamarix habitat areas such as orchards had the potential to be misclassified as saltcedar. However, *Tamarix* primarily grows only along the riparian corridor adjacent to the flood plane. Thus, large rectangular orchard areas were masked out from image classification in order to improve the classification process. After orchard exclusion, accuracy assessment was analyzed using independent field validation data. For producer's accuracy, random samples were selected from the classified tamarix cover class. A differential field GPS unit was then used to locate specific areas where pixels were identified as saltcedars by the proposed classifiers. A field crew located appropriate points and made on-site determination as to whether saltcedar was present or absent at each site. As the majority of the saltcedar in this location are medium to large shrubby trees comprised of several square meters of cover area, the submeter GPS accuracy was considered adequate for this assessment along with aerial photograph-based maps that allowed individual tree recognition in the field. For user's accuracy assessment, we randomly located tamarix patches in the field. The coordinates of these locations were then measured and the sample sites were then compared with the classified tamarix covers back in the laboratory where we verified how many samples were found on the classification map to calculate user's accuracy. Based on the calibrated and verify mapping of tamarix cover, the full area of invasive tamarix within our study area was estimated.

3. Results and Analysis

3.1. Original data analysis

Using twenty sampled pixels with three replications (60 total samples), all eight cover types were compared for their gray-level values. Statistically, there were high correlations among the three scanned color layers in each image. Correlation

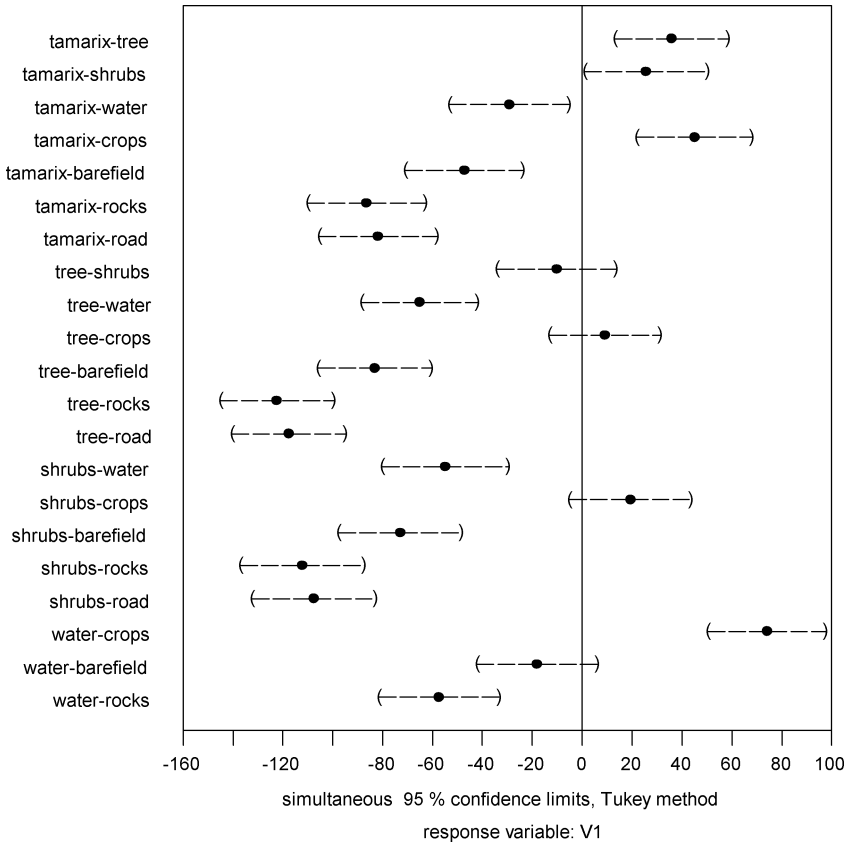

Figure 4. Comparisons on separabilites of different covers by color composition.

coefficients of the first layer versus the second and the third layers was 0.96 and 0.92, respectively. Therefore, to reduce the information redundancy, we only used the blue layer to compare the gray-level difference of covers and derive the texture features. Using analysis of variance, it was determined that there was significant difference at the overall level, however, there existed tonal confusion among some covers. The Turkey multi-comparison demonstrated that some covers partly overlap, which led to confusion in image classification (Figure 4). For example, tamarix sometimes was confused with water and other shrubs, because of their color similarity and spatial overlap where some mixing occurred within the 1 meter pixels. Only when differences were far from the zero separation line, were these covers easily separated. Therefore, just using gray-level or color alone, it was difficult to separate the tamarix from some other shrubs and water. There was also some overlap of gray level among trees, shrubs and crops. *Tamarix* therefore was not significantly different from shrubs, trees, or even water bodies. Clearly it was impossible to distinguish tamarix from its associated vegetation and background using color alone, at this level of spatial resolution.

3.2. Effects of window sizes on separability

Window size provided a functional range of texture features. The separability of the original images was just 1.81 using the overall average. The separability of *Tamarix* from other covers was 1.88. The separability between *Tamarix* and water was only 1.03. When textures were combined with the original data, the separability was significantly improved between different cover types. To some extent, the level of change depended partly on the window size (Tables I–IV). Therefore, window size played an important role in capturing spatial pattern information to improve separability among covers. If a window size is too small, some spatial information contained in larger-scale patterns might be lost. However, if a window size is too large, small cover patterns would be mixed with other patterns. Also, the effect of a texture function may be influenced by window size. For example,

TABLE I
Texture separabilities comparison with $3 * 3$ windows

	Overall separability				*Tamarix* separability			
Textures	Max.	Min.	Average	Covers of Min. separability	Max.	Min.	Average	Covers of Min. separability
Raw	2.00	1.03	1.81	Rocks-roads	2.00	1.03	1.88	Tamarix-water
Hom	2.00	1.20	1.91	Trees-shrubs	2.00	1.56	1.91	Tamarix-water
Mean	2.00	1.15	1.89	Tamarix-waters	2.00	1.15	1.89	Tamarix-water
Con	2.00	1.29	1.95	Trees-shrubs	2.00	1.76	1.95	Tamarix-shrubs
Dis	2.00	1.29	1.95	Trees-shrubs	2.00	1.78	1.94	Tamarix-water
SD	2.00	1.29	1.96	Shrubs-trees	2.00	1.91	1.98	Tamarix-trees
Entropy	2.00	1.30	1.91	Shrubs-trees	2.00	1.48	1.97	Tamarix-trees

TABLE II
Texture separability comparison with $5 * 5$ windows

	Overall separability				*Tamarix* separability			
Textures	Max.	Min.	Average	Covers of Min. separability	Max.	Min.	Average	Covers of Min. separability
Raw	2.00	1.03	1.81	Rocks-roads	2.00	1.03	1.88	Tamarix-water
Hom	2.00	0.95	1.87	Tamarixs-water	2.00	0.95	1.87	Tamarix-water
Mean	2.00	1.30	1.91	Tamarix-water	2.00	1.30	1.91	Tamarix-water
Con	2.00	1.23	1.96	Trees-shrubs	2.00	1.92	1.98	Tamarix-trees
Dis	2.00	1.36	1.95	Rocks-roads	2.00	1.91	1.98	Tamarix-trees
SD	2.00	1.23	1.96	Shrubs-trees	2.00	1.91	1.98	Taamrix-trees
Entropy	2.00	1.43	1.95	Rocks-roads	2.00	1.90	1.96	Tamarix-water

TABLE III
Texture separability comparison with $7 * 7$ windows

	Overall separability				*Tamarix* separability			
Textures	Max.	Min.	Average	Covers of Min. separability	Max.	Min.	Average	Covers of Min. separability
Raw	2.00	1.03	1.81	Rocks-roads	2.00	1.03	1.88	Tamarix-water
Hom	2.00	0.95	1.86	Tamarix-water	2.00	0.95	1.86	Tamarix-water
Mean	2.00	1.28	1.90	Tamarix-waters	2.00	1.28	1.90	Tamarix-water
Con	2.00	1.24	1.96	Nonevergreen trees-shrubs	2.00	1.92	1.98	Tamarix-nonevergreen trees
Dis	2.00	1.36	1.94	Nonevergreen Trees-shrubs	2.00	1.91	1.98	Tamarix-nonevergreen trees
SD	2.00	1.29	1.96	Shrubs-nonevergreen Trees	2.00	1.91	1.98	Tamarix-nonevergreen trees
Entropy	2.00	1.33	1.93	Shrubs-nonevergreen trees	2.00	1.83	1.94	Tamarix-nonevergreen trees

TABLE IV
Texture separability comparison with $9 * 9$ windows

	Overall separability				*Tamarix* separability			
Textures	Max.	Min.	Average	Covers of Min. separability	Max.	Min.	Average	Covers of Min. separability
Raw	2.00	1.03	1.81	Rocks-roads	2.00	1.03	1.88	Tamarix-water
Hom	2.00	1.15	1.93	Nonevergreen trees-shrubs	2.00	1.86	1.96	Tamarix-water
Mean	2.00	1.22	1.89	Tamarix-water	2.00	1.22	1.86	Tamarix-water
Con	2.00	1.26	1.95	Nonevergreen trees-shrubs	2.00	1.88	1.97	Tamarix-water
Dis	2.00	1.31	1.96	Nonevergreen trees-shrubs	2.00	1.91	1.98	Tamarix-Nonevergreen trees
SD	2.00	1.29	1.96	Shrubs-nonevergreen trees	2.00	1.91	1.98	Tamarix-Nonevergreen trees
Entropy	2.00	1.30	1.92	Shrubs-nonevergreen trees	2.00	1.72	1.92	Tamarix-water

the mean texture decreased separability in large window sizes. On the other hand, entropy increases the separability in large window sizes. For the $3*3$ window, the overall average separability was improved from 1.81 to the range of 1.89–1.96; and the *Tamarix* separability was improved to 1.89–1.98. At this window size, the standard deviation improved separability the most. For the $5*5$ window, the overall average separability was improved to 1.87–1.96, while the average separability of *Tamarix* from other covers was improved to 1.83–1.98. The $7*7$ and $9*9$ window sizes had similar effects, but the corresponding separabilities were a little lower than that of the $5*5$ window. Therefore, the $5*5$ window size was finally chosen as the optimal window size for analysis and was then used to extract texture features with these photographs, and was set as the standard window size in all texture measurements along the Cache Creek. These textures were then applied to classify all the images, the images were then mosaiced and used for mapping the saltcedar and estimating overall area of infestation. Among different texture features, those measuring heterogeneity such as the standard deviation and dissimilarity played a more important role in improving separability than the other measures discussed. Based on an overall average and the specific separability of *Tamarix* compared to other classes, the two homogeneity measures gave the poorest performance.

3.3. THE DETERMINATION OF THE OPTIMAL TEXTURE ALGORITHM

The overall accuracy and the specific accuracy for *Tamarix* (Table V) were used to determine the optimal texture for detection and classification of invasive saltcedar across large areas along Cache Creek. A high separability did not necessarily correspond to high accuracy in all categories, but was true for saltcedar cover detection as follows. The overall accuracy was calculated for all eight covers from different textures for comparison with the raw image data. The accuracy for *Tamarix* was singled out separately from other classes as this was the target species of most importance in our analysis. The overall accuracy and accuracy for *Tamarix* across different wondow sizes were sometimes inconsistent. For instance, the dissimilarity

TABLE V
Accuracy assessment of the classification with $5*5$ window size

	Average accuracy	Overall accuracy	Tamarix accuracy	Min. accuracy	Target of Min. accuracy	Max accuracy	Target of Max. accuracy
Raw	90.99	91.38	87.92	78.49	Nonevergreen trees	99.46	Bare fields
Con	93.46	94.74	98.61	88.81	Roads	99.37	Bare fields
Dis	93.72	95.34	84.95	86.17	Nonevergreen trees	100.00	Bare fields
SD	94.37	95.58	97.43	80.79	Roads	100.00	Bare fields
Entropy	96.70	97.41	98.22	87.34	Nonevergreen trees	100.00	Bare fields

texture with a $3 * 3$ window size led to a very high overall accuracy; however, the corresponding saltcedar accuracy was poor. Therefore, the best texture algorithm was judged by balancing among the average, maximum and minimum accuracies for both overall separability and for *Tamarix* separability. For most of the images, the contrast texture was the best choice for saltcedar mapping. Therefore, it was included in all image classification processes. Although the degree of improvement in separability may vary from photograph to photograph due to topography and light conditions, it was shown that texture analysis always improved invasive cover detection, and that consecutive images usually shared the same optimal texture set (Table VI).

3.4. Post processing editing and accuracy assessment

Tamarix, as the focal cover type, only exists along or near creeks. However, in the initial classification, some orchards were also classified as *Tamarix* due to similar bloom characteristics. *Tamarix* was also occasionally confused with shrubs and trees in the riparian zone, but rarely. Based on its habitat characteristics, upland areas where orchards occur and cause apparent classification errors, were corrected and edited as non-invasive covers, and thus the classification results were further improved. In addition, three other non-objective covers (roads, rocks, and bare fields) were merged together for final assessment and analysis. These post-classification processed images were then mosaiced with increased accuracy for final assessment and field use.

To estimate producer's accuracy, we first randomly sampled 400 pixels from classified *Tamarix* covers along the creek. However, most of these points were inaccessible, due to water bodies blocking and steep banks limiting access. A total of 95 sample points were reached in the field. Among these, 74 samples were verified to be *Tamarix* cover (accuracy was 77.89%). Only 12 misclassified pixels were caused by difficulties in separating the classes with the color and texture methods used in the analysis. For example, there were 4 willow pixels classified as saltcedar. There were other objective factors causing some errors that we hope to eliminate in future assessments. For example, there were 5 sample points classified as *Tamarix* that were removed at the time of the field verification, because it was found that there were dead patches of saltcedar around specific sample locations where local landowners had chemically treated and killed these plants. There were also 4 errors in the samples caused by georeferencing problems along steep slopes, for example, near a dam, extreme creek banks, or uneven road edges. For user's accuracy assessment, we used a differential submeter GPS to collect 157 randomly selected field points where saltcedar occurred in patches along the creek. These samples were then checked and compared with the classified saltcedar covers back in the laboratory. There were 112 samples classified as *Tamarix*; however, there were 45 samples not found as tamarix in the map. The resulting user's accuracy was 71.33%. In this case, it was found that the misclassification was caused to some

TABLE VI
The optimal texture measure with different photographs

Photo No.	UTM coordinates	Texture	Photo no.	UTM coordination	Texture
1	605535E, 4288576N 608430E, 4285739N	DEV	16	576180E, 4289000N 580283E, 4284835N	CON
2	603344E, 4288607N 606494E, 4285566N	DEV	17	574660E, 4290559N 578809E, 4286403N	CON
3	601775E, 4289077N 605690E, 4285193N	CON + DEV	18	573141E, 4294140N 577164E, 4288138N	CON
4	600170E, 4287628N 604096E, 4283738N	CON	19	572622E, 4292646N 576464E, 4288832N	CON
5	598642E, 4286268N 602592E, 4282305N	CON	20	571687E, 4294644N 575469E, 4290885N	CON
6	594683E, 4284239N 598181E, 4280859N	CON	21	570776E, 4296627N 574429E, 4293042N	CON
7	592608E, 4284969N 596098E, 4281569N	CON	22	569786E, 4298835N 573439E, 4294552N	CON
8	590332E, 4285671N 593838E, 4282197N	CON	23	568570E, 4300738N 572346E, 4296928N	–
9	588410E, 4286137N 591860E, 4282713N	DIS + DEV	24	567690E, 4302862N 571462E, 4299014N	–
10	586529E, 4286626N 590029E, 4283206N	CON + DIS + DEV	25	566908E, 4303654N 570825E, 4300572N	–
11	584459E, 4287248N 587874E, 4283773N	DEV	26	566424E, 4304561N 570175E, 4301795N	CON
12	583178E, 4287125N 586253E, 4284205N	DEV	27	565631E, 4306054N 569296E, 4302458N	CON
13	581129E, 4286824N 584054E, 4283989N	CON	28	564882E, 4306530N 568845E, 4302605N	CON
14	579046E, 4286667N 582038E, 4283782N	–	29	563348E, 4307980N 567205E, 4304042N	CON
15	577736E, 4287528N 581816E, 4283467N	CON		581816E, 4283467N	

Note: "–" not using any texture.

degree by the spread of this invasive species after the photos were taken or small patch sizes that may not have been easily visible in the 1 meter pixels. These photos were taken in 2001, but the retrospective analysis and final accuracy assessment were not completed until the summer of 2004. Although saltcedar is a relatively slow growing shrub, the three-year time delay certainly added to this error. In all, we found that there were 13 misclassified samples near big patches of saltcedar on the photos in 2001 that could have been caused by *Tamarix* dispersal after the photos

were taken. If these samples were checked in 2001, the corresponding accuracy would certainly have been higher. If we exclude these 13 samples for the accuracy assessment, then the accuracy would have been 77.78%. In the future, in order to have more exact invasion information, the invasive map should be updated and verified each year. It was also determined that 32 samples of isolated saltcedar were not found on the resulting classification map. Such errors were mainly caused by small patches of saltcedar. These small infestation areas were not easy to capture in the image analysis process due to our 1 meter pixel resolution and the texture analysis conducted in the relatively large $5 * 5$ window size. This might be improved by conducting the analysis under finer image resolution, however, constraints of image processing and handling made that level of detail in the analysis impractical and cost prohibitive. Finally, using these analyses and assessing the overall classified *Tamarix* cover along a 40 km section of Cache Creek, the total area of invasive saltcedar was estimated to be 396 hectares (3.96 km^2 Table VII).

It was found that there were many more saltcedar invaded areas in the middle section of the creek and that the invaded areas in up-stream section were less in area and less dense. Through correlation analysis, it was found that the invasive areas were strongly linked with bare soil areas of and water adjacent to the creek (including wetland) (Table VIII). Saltcedar infestation negatively correlates with the amount of bare field area, and positively with the area flooded by water. In the middle section, the area of water in the creek is large but the water flow is slow.

TABLE VII
Invasive characteristics in different parts along Cache Creek in 2001

Creek parts	Tamarix areas (Square meters)	Length of water Body (Meter)	Invasive degree (Square meters / meter)
Down stream	522680	13066	40.00
Middle part	918540	13600	67.54
Up stream	521087	14430	36.11

TABLE VIII
Correlation coefficients among different cover types

	Tamarix	Evergreen	Non-evergreen (including shrubs)	Crops	Bare fields	Water bodies (including wetland)
Tamarix	1.00	−0.58	−0.77	0.47	−0.99	0.96
Evergreen		1.00	0.97	−0.99	0.69	−0.78
Non-evergreen			1.0000	−0.93	0.85	−0.92
Crops				1.00	−0.59	0.70
Bare fields					1.00	−0.99
Water bodies						1.00

Possibly, such water condition forms a habitat condition beneficial to saltcedar seed germination and invasion along the creek The invasion of *Tamarix* also competitively reduces native vegetation in infested areas leading to a further negative correlation with both evergreen and non-evergreen plant covers in these areas.

4. Discussion

Previous studies of invasive plant species detection using remote sensing and image analysis have primarily emphasized the use of reflectance or color properties alone. In those studies results have provided some but limited success. In situations where effective detection has been achieved, it has been attributed to substantial differences in reflectance caused by changing phenological characteristics between the species of interest and the associated environment (Everitt and Deloach, 1990; Everitt *et al*., 1995; Lass *et al*., 1996). In this research, color differences from natural color photographs were not sufficiently large between the invasive target species and other associated background vegetation to allow accurate classification. Texture analysis increased the separability between invasive cover and these background plants and other habitat features.

We intended to find proper texture(s) from six different measures. In fact, the spatial dispersion patterns in plant ecology are typically scale-dependent, and thus we hoped to find an appropriate texture measure to describe the spatial pattern of gray levels of a pixel neighborhood at different scales of study. That is, after evaluating several different scales (different window sizes), we applied the optimal texture assessment to extract the spatial neighbor relationships with a particular window size (5×5 pixels). This texture was then used as an additional layer in image classification and improved the average separability (minimum accepted value set to 1.90). However, occasionally in some images, a selected window size, using only one texture did not reach a separability of over 1.90. Thus we included two or three different texture measurement to capture the optimal texture for comparison and thus ensured that the separability was always greater than 1.90.

Sometimes the separability improvement was not much different among textures producing similar results as seen in the contrast and dissimilarity texture measures. The optimal texture assessment method could only be determined after the full accuracy assessment was completed, and it was expected to have a higher overall accuracy and the best accuracy for the specific classification of *Tamarix*. During this process, we also assessed the use textures other than the selected optimal texture(s) to improve classification accuracy. In the assessment process, we found that none of the other textures increased accuracy more than 2%, even when using all six texture measures simultaneously to do the classification. Therefore in the end, we used the optimal texture subset alone, instead of all the texture measures combined to extract the *Tamarix* cover. These results suggest that gray-level values of digitized photographs in combination with a single texture feature can be effectively used

in an automatic procedure to detect invasive *Tamarix* in large areas of infestation. Such detection is possible for not only large tracts of invasive areas but also for small patches where local land managers are interested in detecting and eradicating these plants.

5. Conclusions

In this study, we demonstrated that texture could be used to improve the separability between invasive *Tamarix parviflora* and associated vegetation along an example riparian corridor in California. Texture features were useful in developing a relatively automatic procedure for detection and recognition of *Tamarix* using historical color aerial photographs. We derived six different texture algorithms from a gray-level co-occurrence matrix (GLCM), which proved useful for improving classification results. The optimal window size was 5×5 among 4 other bracketing window sizes. This optimal size was chosen based on the separability of cover types with special attention paid to the separability of *Tamarix* when compared to other cover types. The producer's and user's accuracies were found to be 77.89% and 71.33%, respectively. Totally, there was 396 hectares (3.96 km^2) of *Tamarix* cover along the invaded Cache Creek drainage.

Acknowledgments

We are grateful to Dr. Ruiliang Pu for his help on the use of PCI software and discussions on the application of remote sensing for use in mapping invasive species. We also thank Mr. Justin Weber, Mr. Joel Garza and Ms. Julie Garren for their field validation work. In particular, we thank USDA-ARS # 5325-22000-017-00D (Biology and Control of invasive weeds on the Western United States) and USDA-CSREES-IFAFS # 00-52103-9647 (Biologically-based control for the area-wide management of exotic and invasive weeds).

References

Anys, H. and He, D. C.: 1995, 'Evaluation of textural and multipolarisation radar features for crop classification', *IEEE Trans. on Geosci. Remote Sens.* **33**, 1130–1181.

Bailey, Joseph K., Schweitzer, J. A. and Whitham, T. G.: 2001, 'Salt cedar negatively affects biodiversity of aquatic macroinvertebrates', *Wetlands* **21**, 442–447.

Brock, J. H.: 1994, '*Tamarix* spp. (Salt Cedar), An Invasive Exotic Woody Plant in Arid and Semi-arid Riparian Habitats of Western USA', In: L. C. de Waal, L. E. Child, C. P. M. Wade, J. H. Brock, *Landscape Ecology Series; Ecology and Management of Invasive Riverside Plants*, John Wiley and Sons Ltd.; John Wiley and Sons, Inc.; Chichester, UK/New York, USA, 1994, pp. 27–44.

Cleverly, J. R., Smith, S. D., Sala, A. and Devitt, D. A.: 1997, 'Invasive capacity of *Tamarix ramosissima* in a Mojave desert floodplain: The role of drought', *Oecologia* (Berlin) **111**, 12–18.

Di Tomaso, J. M.: 1998, 'Impact, biology and ecology of saltcedar (*Tamarix* spp.) in the southwest United States', *Weed Tech.* **12**, 326–336.

Everitt, J. H. and Deloach, C. J.: 1990, 'Remote sensing of Chinese Tamarisk (*Tamarix chinensis*) and associated vegetation', *Weed Sci.* **38**, 273–278.

Everitt J. H., Escobar, D.E. and Davis, M. R.: 1995, 'Using remote sensing for detecting and mapping noxious plants', *Weed Abstr.*, **44**, 639–649. CAB internal.

Everitt, J. H., Escobar, D. E, Alaniz, M. A, Davis, M. R. and Richardson, J. V.: 1996, 'Using spatial information techniques to map Chinese tamarisk (*Tamarix chinensis*) infestations', *Weed Sci.* **44**, 194–201.

Gausman, H. W., Everitt, J. H., and Gerbermann Bowen R. L.: 1977, 'Canopy reflectance and film image relations among three south Texas rangelands plants', *J. Range Manage.* **30**, 449–450.

Gong, P., Marceau, D. J. and Howarth, P. J.: 1992, 'A comparison of spatial feature extraction algorithms for land-use classification with SPOT HRV data', *Remote Sens. Environ.* **40**, 137–151.

Haralick, R. M.: 1979, 'Statistical and structural approaches to texture', *Proc. IEEE*, **67**, 786–804.

Haralick, R. M., Shanmugam, K. and Dinstein, I.: 1973, 'Textural features for image classification', *IEEE Tran. Geosci. Remote Sens.* **33**, 1170–1181.

Hassan, A. and He, D. C.: 1995, 'Evaluation of textural and multi-polarization radar features for crop classification', *IEEE Tran. Geosci Remote Sens.* **33**, 1170–1181.

Hudak, A. T. and Wessman C. A.: 1998, 'Textural analysis of historical aerial photography to characterize woody plant encroachment in South African Savanna', *Remote Sens. Environ.* **66**, 317–330.

Jonathan, C.-W. C., Defries, R. S. and Townsend, R.G.: 2001, 'Improved Recognition of Spectrally Mixed Land Cover Classes Using Spatial Textures and Voting Classifications', CAIP 2001, LNCS 2124, 217–227.

Lass, L. W., Carson, H. W. and Callihan, R. H.: 1996, 'Detection of yellow starthistle (Centaurea solstitialis) and common St. Johnswort (Hypericum perforatum) with multispectral digital imagery', *Weed Tech.* **11**, 248–256.

Mather, P. M., Tso, B. C. K. and Koch, M.: 1998, 'An evaluation of Landsat TM spectral data and SAR –Derived textural information for Litho logical discrimination in the Red Sea Hills, Sudan', *Int. J. Remote Sens.* **19**, 587–604.

Nyoungui, A. N., Tonye, E. and Akono, A.: 2002, 'Evaluation of speckle filtering and texture analysis methods for land covers classification from SAR images', *Int. J. Remote Sens.* **23**, 1895–1925.

Podest, E. and Saatchi, S.: 2002, 'Application of multiscale texture in classifying JERS-1 radar data over tropical vegetation', *Int. J. Remote Sens.* **23**, 1487–1506.

Riou, R. and Seyler, F.: 1997, 'Texture analysis of tropical rain forest infrared satelliate images', *PE and RS*. **63**, 515–521.

Saatchi, S. S., Nelson, B., Podest, E. and Holt, J.: 2000, 'Mapping land cover types in the Amazon Basin using 1 km JERS-1 mosaic', *Int. J. Remote Sens.* **21**, 1183–1200.

Shaban,M. A. and Dikshit, O.: 2001, 'Improvement of classification in urban areas by the use of textural features: The case study of Lucknow city, Uttar Pradesh' *Int. J. Remote Sens.* **22**, 565–593.

Smits, P. C. and Annoni, A.: 1999, 'Updating Land-cover maps by using texture information from very high-resolution space-borne imagery', *IEEE Trans. Geosci. Remote Sens.* **37**, 1244–1254.

Stohlgren, T. J., Binkley, D., Chong, G. W. Kalkhan, M. A., Schell, L. D., Bull, K. A. Otsuki, Y., Newman, G., Bashkin, M. and Son, Y.: 1999, 'Exotic plant species invade hot spots of native plant diversity', *Ecol. Mon*og. **69**: 25–46.

Xu, B., Gong, P., Spear R. and Seto, E.: 2003, 'Comparison of different gray level reduction schemes for a revised texture spectrum method for land-use classification using IKONOS imagery', *PE. RS*. **69**, 529–536.

Zavaleta, E.: 2000, 'The economic value of controlling an invasive shrub', *Ambio* **29**, 462–467.